HGG Advances

ARTICLE

A cross-ancestry genome-wide meta-analysis, fine-mapping, and gene prioritization approach to characterize the genetic architecture of adiponectin

Vishal Sarsani,[1] Sarah M. Brotman,[2] Yin Xianyong,[3] Lillian Fernandes Silva,[4] Markku Laakso,[4] and Cassandra N. Spracklen[5,6,*]

Summary

Previous genome-wide association studies (GWASs) for adiponectin, a complex trait linked to type 2 diabetes and obesity, identified >20 associated loci. However, most loci were identified in populations of European ancestry, and many of the target genes underlying the associations remain unknown. We conducted a cross-ancestry adiponectin GWAS meta-analysis in ≤46,434 individuals from the Metabolic Syndrome in Men (METSIM) cohort and the ADIPOGen and AGEN consortiums. We combined study-specific association summary statistics using a fixed-effects, inverse variance-weighted approach. We identified 22 loci associated with adiponectin ($p < 5 \times 10^{-8}$), including 15 known and seven previously unreported loci. Among individuals of European ancestry, Genome-wide Complex Traits Analysis joint conditional analysis (GCTA-COJO) identified 14 additional distinct signals at the *ADIPOQ*, *CDH13*, *HCAR1*, and *ZNF664* loci. Leveraging the cross-ancestry data, FINEMAP + SuSiE identified 45 causal variants (PP > 0.9), which also exhibited potential pleiotropy for cardiometabolic traits. To prioritize target genes at associated loci, we propose a combinatorial likelihood scoring formalism (Gene Priority Score [GPScore]) based on measures derived from 11 gene prioritization strategies and the physical distance to the transcription start site. With GPScore, we prioritize the 30 most probable target genes underlying the adiponectin-associated variants in the cross-ancestry analysis, including well-known causal genes (e.g., *ADIPOQ, CDH13*) and additional genes (e.g., *CSF1*, *RGS17*). Functional association networks revealed complex interactions of prioritized genes, their functionally connected genes, and their underlying pathways centered around insulin and adiponectin signaling, indicating an essential role in regulating energy balance in the body, inflammation, coagulation, fibrinolysis, insulin resistance, and diabetes. Overall, our analyses identify and characterize adiponectin association signals and inform experimental interrogation of target genes for adiponectin.

Introduction

Adiponectin, an abundant adipocytokine secreted almost exclusively by adipocytes, is crucial in the interconnection between adiposity, insulin resistance, and inflammation.[1–3] Previous genetic studies have identified more than 20 loci harboring variants associated with serum levels of adiponectin, including *ADIPOQ* (OMIM: 605441) and *CDH13* (OMIM: 601364).[4–7] Genetic analyses have also indicated shared allelic architecture between adiponectin, type 2 diabetes (OMIM: 125853), and other metabolic traits (e.g., body mass index [BMI], waist-hip ratio [WHR]).[4,7,8] Due to its diverse physiological functions in glucose and lipid metabolism, inflammation, and oxidative stress across metabolic and cardiovascular tissues, adiponectin could be a possible therapeutic target for metabolic syndrome, diabetes, and coronary disease.[9] However, to move established loci toward effective clinical and therapeutic targets, the functional variant(s), target/effector gene(s), and the mechanistic direction(s) of effect need to be identified; for most loci identified to date, this information remains largely unknown.

Multiple methods have been proposed to prioritize target genes underlying genome-wide association study (GWAS) signals using expression, functional genomics, and network data.[10–12] However, individual approaches often have conflicting findings, making it difficult to interpret or prioritize candidate target genes. Attempts to incorporate integrative and complementary gene prioritization approaches to identify disease-risk genes have been somewhat successful.[13,14] However, the primary challenge in using prioritization approaches for a complex trait or disease is that the lack of customizability to focus on the integration of the data that are most relevant (e.g., tissue specificity) to the disease or trait of interest. This may result in a researcher choosing results in an *ad hoc* or *post hoc* manner. A researcher may also want to maximize the likelihood of selecting a suitable target gene for experimental follow-up, and considering support from multiple approaches will make the selection(s) more robust.

Leveraging summary statistics from diverse genetic studies, we conducted a cross-ancestry, genome-wide meta-analysis for adiponectin in up to 46,434 individuals from the Metabolic Syndrome in Men (METSIM) cohort

[1]Department of Mathematics and Statistics, University of Massachusetts Amherst, Amherst, MA, USA; [2]Department of Genetics, University of North Carolina at Chapel Hill, Chapel Hill, NC, USA; [3]Department of Biostatistics and Center for Statistical Genetics, University of Michigan School of Public Health, Ann Arbor, MI 48109, USA; [4]Institute of Clinical Medicine, Internal Medicine, University of Eastern Finland, Kuopio, Finland; [5]Department of Biostatistics and Epidemiology, University of Massachusetts Amherst, Amherst, MA, USA
[6]Lead contact
*Correspondence: cspracklen@umass.edu
https://doi.org/10.1016/j.xhgg.2023.100252.

and the Adiponectin Genetics (ADIPOGen) and Asian Genetic Epidemiology Network (AGEN) consortiums.[4,5,15] Our primary objectives were to (1) discover previously unreported loci associated with plasma adiponectin levels, (2) narrow putative causal variants underlying the association signals, (3) prioritize target genes systematically by using our proposed Gene Priority Score (GPScore) approach based on evidence derived from 11 gene prioritization strategies and physical distance to transcription start sites, and (4) perform functional profiling of target genes and their underlying pathways.

Material and methods

Ethics statement

The research protocol for all studies was reviewed and approved by the institutional ethics review committees at the involved institutions. Written informed consent was obtained from all study participants.

Study design and participants

Our meta-analysis included summary statistics from 16 studies of European-ancestry individuals from the ADIPOGen consortium (n = 29,347 from the discovery phase),[4] four studies with individuals of East Asian ancestry from the AGEN consortium (n = 7,825),[5] and the METSIM study (European ancestry; n = 9,262).[15] While most of our analyses were performed in both European-only and all ancestries combined ("cross-ancestry"), we consider the cross-ancestry analyses to be our primary results. A detailed description of participant characteristics, genotype and phenotype information, quality control, and imputation can be found in Table S1.

Genome-wide meta-analyses

We performed the European-ancestry and cross-ancestry adiponectin meta-analyses using a fixed-effects inverse variance-weighted meta-analysis approach with the random-effects model (RE2) implemented in METASOFT,[16] which corrects for population structure while allowing for examination of heterogeneity statistics. In the cross-ancestry meta-analysis, we also generated Bayes factors (BFs) from MR-MEGA,[17] which employs meta-regression to account for heterogeneity in allelic effects associated with ancestry. We defined the "lead" association signal at each locus to be the most significant variant ($p < 5 \times 10^{-8}$) within a 500-kb window. We considered association signals to be previously unreported, or "additional," if they were located >500 kb from a previously reported adiponectin signal. To identify distinct association signals at each locus identified in the European-ancestry analysis,[4–6,15,18] we performed approximate conditional analyses using genome-wide joint conditional analysis (COJO) implemented in the Genome-wide Complex Traits Analysis (GCTA) software.[19] Using data from 10,197 METSIM participants to calculate linkage disequilibrium (LD) and a collinearity threshold of $(R^2) = 0.9$, we considered a variant to represent an additional, distinct signal at a locus if (1) the variant achieved ($p < 5 \times 10^{-8}$) in the COJO analysis, and (2) the variant was located within ±1 Mb from the original lead variant at that locus. We use "index variant" to denote the most significant variant within each of the secondary association signals.

Replication analyses

Index variants at all 22 loci identified in the cross-ancestry analysis were interrogated for replication in an independent sample data of 35,559 Icelanders from deCODE genetics.[20] Within deCODE, plasma protein levels of adiponectin were measured using the SomaScan v4 proteomics platform. Results were available for 21 of the index variants; results were meta-analyzed with those from ADIPOGen, METSIM, and AGEN using fixed-effects models.

Pleiotropic associations with phenotypes from CMDKP

We interrogated our lead and index variants with data from the Common Metabolic Diseases Knowledge Portal to explore pleiotropic associations between the index variants from the cross-ancestry meta-analysis and other complex traits across five common disease areas (type 1 and type 2 diabetes, cardiovascular and cerebrovascular disease, and sleep disorders). We only considered traits/diseases that achieved $p < 0.05$ in the original analyses. For ease of visualization, we aggregated traits/diseases into 23 broad categories.

Identifying candidate causal variants

We used several approaches to identify candidate causal variants at loci identified in both the cross-ancestry and European-ancestry-only meta-analyses. Unless otherwise stated, we used data from 10,197 METSIM participants as the reference for LD calculations.

Statistical fine-mapping

We performed statistical fine-mapping using FINEMAP[21] and SuSiE.[22] At each adiponectin-associated locus, we computed in-sample dosage LD using LDstore.[23] We defined a fine-mapping region as the 3-Mb window (±1.5 Mb) around each lead variant. This window size is based on recommendations for fine-mapping and colocalization (coloc) analyses, especially when working with diverse populations.[24,25] We allowed up to 10 causal variants per window and extracted the posterior inclusion probabilities (PIP) of each variant using each method independently. The variants with a PIP > 0.90 in either of the fine-mapping methods, along with having LD $r^2 > 0.8$ with the lead variant, are considered the final candidate causal variants. We conducted an analysis of suspicious loci for cross-ancestry fine-mapping using the SLALOM method.[26] To identify outlier variants and suspicious loci, we set the following criteria: $r^2 > 0.8$ and $P_{\mathrm{DENTIST-S}} < 1.0 \times 10^{-4}$, where $P_{\mathrm{DENTIST-S}}$ is a metric for detecting errors in the analyses of summary statistics.[27]

Causal variant annotation

The majority of the candidate causal variants reside in non-coding regions of the human genome. We used RegulomeDB[28] to annotate the candidate causal variants from fine-mapping with evidence of regulatory function(s) through functional genomic assays and computational approaches. RegulomeDB provides a score (range 1–7) indicating its potential to be functional in regulatory elements and the probability of confidence in the score for each variant. We interrogated fine-mapped candidate causal variants from the cross-ancestry fine-mapping using CAUSALdb,[29] a database containing fine-mapping results from over 3,052 GWAS summary statistics. Whenever multiple variants mapped to the same trait across different studies, we meta-analyzed the different p values together.

Gene prioritization

We created the GPScore, which combines evidence from 11 gene prioritization strategies,[11,22,30–38] along with the physical distance to the transcription start sites (TSSs), to prioritize target genes underlying our adiponectin association signals. For all approaches, we considered all protein-coding genes within ±1.5 Mb of the original lead variant from the multi- or European-ancestry meta-analyses. For prioritization solely based on gene expression,[22,32–35] we restricted our analysis to tissues most biologically relevant to adiponectin (adipose subcutaneous, adipose visceral omentum, adrenal gland, artery

aorta, artery coronary, artery tibial, heart atrial appendage, heart left ventricle, kidney cortex, liver, muscle-skeletal, thyroid, and whole blood). Unless otherwise stated, we used data from 10,197 METSIM participants as the reference for LD calculations, and default settings were used for gene prioritization strategies.

Gene prioritization score

GPScore is a combinatorial likelihood score constructed by leveraging various gene prioritization strategies described below. The score can be customized to include weighting factors to prioritize signals from a particular tissue. GPScore is defined as

$$GPScore = \frac{(-Log_{10}(P_G) + S_G).C_S}{log_2 TSS_d}$$

where p_G is a combined p value for MAGMA,[30] summary Mendelian randomization (SMR),[33] expression quantitative trait loci (eQTLs) coloc (LD-based approach), SNP-heritability enrichment,[34] and Downstreamer[37] (described below), computed by the sum of z via Stouffer's method.[39] The second term (S_G) represents the combined scores of eQTL coloc,[40] EMS,[35] polygenic priority score (PoPS),[36] epigenome integration across multiple annotation projects (EpiMap),[11] combined SNP-to-gene (cS2G),[38] and GeneHancer[18] scores. Each of the scores from EMS, PoPS, and Genehancer was independently normalized by scaling its values between 0 and 1. The terms p_G and S_G capture the strength of associations for a gene depending on the output of a tool. The third term (C_S) is a score ranging from 0 to 1, representing the proportion of support for a particular protein-coding gene across all 11 gene prioritization strategies. Each strategy has a maximum support score of 1. For eQTL colocs, SNP-heritability enrichment, EMS score, and SMR, we assigned a score of 1 if the tissue source was adipose or cardiac-related tissue (given the trait of interest is adiponectin); otherwise, we assigned a score of 0.8. The final term (TSS_d) is the distance from the lead variant to the transcription start site of the gene/transcript, measured in base pairs, and is intended to penalize genes that are far away from the lead variant.

One of the methodological issues in computing GPScore is that some of the gene prioritization strategies (i.e., coloc, EMS, SMR, GeneHancer, cs2G) report values for individual variants/position, whereas other strategies prioritize genes (i.e., MAGMA, Downstreamer, EpiMap, PoPS, LDSC). We transformed variant/position-level scores into gene-level scores using recommendations from Lehne et al.[41] For expression-based enrichments, a variant/position may have a statistic corresponding to a tissue (e.g., coloc of a variant in adipose tissue). Using the average or highest quartile of a statistic may result in the inability to assign tissue information after the final transformation. Because preserving tissue information in the variant scores is essential for weighing support (C_S), we have opted to use either the lowest p value (MAGMA, SMR, eQTL coloc LD-based approach, SNP-heritability enrichment, Downstreamer) or the maximum score (coloc, EMS, PoPS, EpiMap, GeneHancer) per gene. Alternatively, in situations where tissue information is less critical, the average or highest quartile of statistics could be used.

Selection of prioritized genes based on GPScore

The top gene for each 3-Mb window (±1.5 Mb around the index variant) was selected based on the highest GPScore value per locus. In addition to this, each gene was evaluated for its biological relevance to the trait under study and for its GPScore consistency relative to the top-scoring gene within the same window. A gene was considered consistent and also selected as a prioritized gene if its GPScore was approximately within one-third (33%) of the top gene's score.

MAGMA gene analysis

To quantify the degree of association of each gene with adiponectin while incorporating LD structure between variants, we used MAGMA v1.10[30] to perform gene-set analyses and obtain gene p values from the multiple linear principal components regression F test. The null hypothesis of the F test is that the gene has no effect on the phenotype, conditional on all covariates. The variant-wise mean model was used, and variants were assigned to one of the 18,383 (GRCh37) protein-coding genes with an annotation window of 50 kb. We used the computed gene p value to calculate the p_G term in GPScore.

eQTL coloc

We used a combination of SuSiE[22] and coloc[32] to assess for evidence of shared association signals/causal variants between our adiponectin GWAS data and *cis*-eQTLs from GTEx[42] using the coloc.susie() function.[40] The coloc + SuSiE approach has been shown to improve the accuracy of coloc analyses (coloc only) when multiple causal variants exist within a window.[40] We extracted the posterior probability of the variant being causal for the shared signal for each tissue most biologically relevant to adiponectin and used it in the S_G term for the GPScore.

eQTL coloc (LD based)

As a supplemental approach to coloc + SuSiE, we further examined for colocs between our adiponectin-associated variants and eQTLs in GTEx and in RNA sequencing (RNA-seq) data from 434 METSIM participants using an LD-based approach.[31] For coloc with the GTEx data (restricted to adiponectin-related tissues described above), we considered the GWAS and eQTL signals to be colocalized when the lead or index GWAS variant and the variant most strongly associated with the expression level of the corresponding transcript (eSNP) exhibited high pairwise LD (LD $r^2 > 0.70$) in European + East Asian ancestry data within 1KGp328. We employed a less stringent LD $r^2 > 0.70$ for cross-ancestry data to account for heterogeneity across populations and to avoid the potential loss of variants due to the "averaging-out" effect. For coloc with the METSIM RNA-seq data, we considered the GWAS and eQTL signals to be colocalized when the lead or index GWAS variant and the eSNP exhibited high pairwise LD (LD $r^2 > 0.80$) calculated using 10,197 METSIM (Finnish) participants. The p value of association with the eSNP was used to calculate the p_G term in GPScore.

SMR

SMR is another approach that integrates GWAS and eQTL data to identify genes whose expression levels are associated with a complex trait. We applied multi-SNP SMR[33] to test for the effect of gene expression (adiponectin-related tissues from GTEx) variation on adiponectin. We included the probes with at least one *cis*-QTL at $P_{EQTL} < 5 \times 10^{-8}$, and we performed a heterogeneity in dependent instruments (HEIDI) test to exclude results that may reflect linkage. In GPScore calculations, we considered the P_{SMR} values of each probe corresponding to tissue, excluding probes with strong evidence of heterogeneity ($P_{HEIDI} > 0.01$). We used the P_{SMR} to calculate the p_G term in GPScore.

SNP-heritability enrichment

To evaluate whether the variant heritability was enriched in the variants within tissue-specific genes (±100 kb) compared to other regions, we applied partitioned LD score regression (LDSC)[34] with the "-overlap-annot" option. We constructed the annotation list of tissue-specific genes by selecting genes with the top 10% median transcripts per million (TPM) values in each adiponectin-relevant tissue from the expression data. We calculated the p values from one-sided Z score coefficients for tissue-specific genes and included them in the p_G term in GPScore.

EMS annotation

The EMS annotation is defined as the predicted probability that a variant has a *cis*-regulatory effect on gene expression, which we calculated by training a random forest model on fine-mapped eQTLs and 6,121 features, such as epigenetic marks and sequence-based neural network predictions.[35] We extracted the computed EMS for all top variant-gene pairs in adiponectin-relevant tissues in GTEx v8[42] from the Finucane Lab. We then extracted the normalized EMS score for all variants from the adiponectin meta-analyses ($p < 0.05$ and minor allele frequency >0.50%) and then incorporated it into the S_G term in GPScore.

PoPS

A gene-level PoPS is a similarity-based gene prioritization approach that leverages both polygenic and locus-specific genetic signals.[36] We used PoPS v0.2 to identify potential target genes from gene-level association statistics (derived from MAGMA) by integrating 57,543 gene features from public bulk and single-cell expression datasets, protein-protein interaction networks, and pathway databases. The PoPs score for each gene is then incorporated into the S_G term in GPScore.

Downstreamer

We used Downstreamer[37] to calculate co-regulation *Z* scores per gene using expression data from 31,499 public RNA-seq samples from many different tissues.[43] Integrating this information into the calculation of the gene priority score will likely prioritize genes that are co-regulated with many important adiponectin-associated genes in the GWAS. We calculated the p values from one-sided co-regulation *Z* scores per gene and included them in calculating the p_G term in GPScore.

EpiMap

Human epigenome reference EpiMap uses the correlation of enhancer activity with gene expression across cell types to map regulatory SNPs to their target genes. This information is useful in the complex trait investigation and studies of disease locus mechanisms. We downloaded gene-enhancer links by mark activity-by-gene expression correlation for the adipose tissue from the EpiMap repository[11] and mapped the link scores for the genes overlapping in the 3-Mb region around the lead variant. We then incorporated the link scores into the S_G term in GPScore.

GeneHancer

GeneHancer calculates a score derived from gene-enhancer genomic distances and combined scores of tissue co-expression correlation between genes and enhancer RNAs, enhancer-targeted transcription factor genes, eQTLs for variants within enhancers, and capture Hi-C.[18] The score represents the strength of enhancer association to a particular gene (GeneHancer score), which can be useful in predicting regulatory elements and their target genes. We extracted the GeneHancer scores for enhancer gene pairs for genes physically located within the adiponectin fine-mapping regions and incorporated them into the S_G term in GPScore.

cS2G score annotation

The cS2G strategy is a heritability-based framework that combines different SNP-to-gene strategies to link regulatory variants to their target genes. We extracted the cS2G scores, which include 10 main functional SNP-to-gene strategies, as previously described,[38] from 9,997,231 variants in the 1000 Genomes Project European reference panel and 19,476,620 variants in the UK Biobank. The cS2G score annotation was performed on selected variants ($p < 0.05$ and minor allele frequency > 0.50%) from the meta-analyses. The cS2G score ranges from 0 to 1, where a score >0.5 is considered good evidence; we incorporated this score into the S_G term in GPScore.

Disease enrichment and functional association networks

Disease enrichment analysis of prioritized genes

To study mechanisms underlying human diseases related to adiponectin, we investigated the human gene-disease associations of our adiponectin-prioritized genes. We examined for enrichment between the prioritized genes from the cross-ancestry adiponectin meta-analysis and a wide range of disease phenotypes relevant in human genomics by gene-disease enrichment analysis (DisGeNET),[44] using enrichr.[45] We considered a DisGeNET term enriched if adjusted $p < 0.01$.

Functional association network construction

To investigate potentially functionally similar genes and their underlying pathways, we constructed a functional association network using GeneMANIA.[46] Prioritized genes alone do not contain enough information to build networks that mediate the underlying functional relationship. We used an algorithm[47] in GeneMANIA that constructs network weights based on the reproducibility of Gene Ontology (GO) biological process co-annotation patterns. We expanded the gene list with functionally similar genes from multiple genomics and proteomics data sources. We primarily used the physical and genetic interaction, predicted protein interaction, and pathway and molecular interaction data available in GeneMANIA.

Results

Cross-ancestry meta-analysis reveals 15 known and seven additional risk loci for adiponectin

We conducted a cross-ancestry, genome-wide association meta-analysis for adiponectin using summary statistics from the METSIM cohort[15] and the ADIPOGen[4] and AGEN consortia[5] ($N \leq 46,434$; Table S1). We also performed a genome-wide association meta-analysis for adiponectin in data from up to 38,609 individuals of European ancestry (METSIM cohort and ADIPOGen consortium only).[4,15] Each individual cohort performed single-variant association analyses for adiponectin, adjusted for age, sex, BMI, and study-specific covariates as appropriate (e.g., principal components, study site). We meta-analyzed summary statistics using fixed-effects analyses implemented in METASOFT.[16] We corrected for population substructure in the cross-ancestry meta-analysis using the computed inflation factors for both the mean effect ($\lambda_{\text{MeanEffect}}$) and heterogeneity portions ($\lambda_{\text{heterogeneity}}$).[16] Because RE2[16] and MR-MEGA[17] are not sufficiently powered in a meta-analysis of only three input files,[48] we consider the fixed-effects results as our primary results; however, we present results from RE2 and MR-MEGA for comparison.

Cross-ancestry

Meta-analysis association results. We identified 22 loci associated with adiponectin ($p < 5 \times 10^{-8}$), including seven loci that have not previously been associated with adiponectin (Table 1; Figures 1 and S1). Previously unreported loci are located at or near *CSF1* (OMIM: 120420), *RGS17* (OMIM: 607191), *ADRB1* (OMIM: 109630), *PDE3B* (OMIM: 602047), *RBMS2* (OMIM: 602387), *HCAR1* (OMIM: 606923), and *PHF23* (OMIM: 612910). Effect direction for all lead variants showed concordance between all three studies, and the effect sizes for each of the lead variants were also consistent between the three datasets

(Spearman $r \geq 0.88$; Figure S2). Further, MR-MEGA results for all 22 loci have a log10BF > 30, further supporting the results from the fixed-effect models. We also confirmed ($p < 0.05$) 83 out of 148 (56.1%) previously reported variants to be associated with adiponectin in our meta-analysis (Table S2).

Lead variants at four loci exhibited evidence of heterogeneity in effect sizes ($I^2 > 80\%$; rs1515108 (*IRS1*; OMIM: 147545), rs17366568 (*ADIPOQ*), rs7978610 (*ZNF664*; OMIM: 617890), and rs12051272 (*CDH13*); Table 1). All four loci are well-established associations with adiponectin levels.[4,5,7] Among the four heterogeneous loci, two of the loci were still considered statistically significant in RE2 models accounting for the high heterogeneity (rs17366568, rs12051272). Large differences in effect allele frequencies between European- and East Asian ancestry populations are likely driving the observed heterogeneity (Table 1 and Figure S2). While it is unknown whether adiponectin levels measured by ELISA are well correlated with those from proteomics panels, we conducted a replication analysis of the index variants using an independent sample data of plasma protein levels of adiponectin from deCODE genetics.[20] Nineteen of 21 (90.4%) index variants (for which data were available) maintained genome-wide significance after meta-analyzing our results with those from deCODE.

European meta-analysis

In a meta-analysis of European-ancestry individuals from METSIM and the ADIPOGen consortium, we identified 19 loci associated with adiponectin (Table 2; Figures 1 and S2), 18 of which were also identified in the cross-ancestry results. One additional previously unreported locus, located near *LINC01214* on chromosome 1 (rs7617025), was identified only in the European-ancestry analysis. All the lead variants showed effect direction concordance between METSIM and ADIPOGen.

Distinct association signals

At all 19 loci identified in the European ancestry, we sought to identify additional association signals located within ±1 Mb of the lead variant using GCTA-COJO. We detected ($p_{joint} < 5 \times 10^{-8}$) 14 additional signals at four loci (Table S3; Figures 1 and S3), including eight signals near *ADIPOQ* (LD r^2 = 0.001–0.846), one near *HCAR1* (LD r^2 = 0.183), one near *ZNF664* (LD r^2 = 0.008), and four near *CMIP*; OMIM: 610112/*CDH13* (LD r^2 = 0–0.046) (Table S4).

Pleiotropic associations with complex traits

We evaluated the lead variants at each of the 22 loci reported in the cross-ancestry meta-analysis for association with other complex traits and diseases. For these traits, we examined existing GWAS and genome-wide meta-analysis results in the Common Metabolic Diseases Knowledge Portal (www.cmdkp.org). We found 89 unique lead variant-phenotype combinations that reached Bonferroni significance (Table S5). Lead adiponectin-associated variants are most strongly associated with the lipids, hepatic, hematological, glycemic, and anthropometric phenotype groups (Figure S4; Table S5).

Putative causal variants implicate shared biological mechanisms

Fine-mapping to identify potential causal variants

To identify potential causal variants underlying adiponectin association signals in both the multi- and European-ancestry analyses, we first constructed 3-Mb windows (±1.5 Mb) around the lead variant (Figure S5). The variants with a PIP > 0.90 in either FINEMAP[21] or SuSiE[22] and LD $r^2 > 0.8$ with the lead GWAS variant were identified as candidate causal variants. In fine-mapping the cross-ancestry adiponectin loci, we nominated 45 putative causal variants at 17 loci (Table S6; Figure S6). Among the 45 putative causal variants, 10 (rs2061155, rs1515108, rs1108842, rs998584, rs596359, rs10787516, rs10886863, rs7978610, rs12051272, rs731839) were also the lead variants from the meta-analysis. In the European-ancestry analyses, fine-mapping analyses nominated putative causal variants at seven loci, including two variants near *CDH13* (Table S7; Figure S7). Among the seven putative causal variants, six (rs16861209, rs998584, rs11045172, rs2925979, rs12051272, rs731839) were the lead variants from the meta-analysis.

Regulatory effects of nominated causal variants

To investigate the regulatory effects among our nominated causal variants, we used the RegulomeDB[28] to obtain RegulomeDB scores, which rank the presence of regulatory motifs for variants on a scale from 1a (most evidence) to 7 (no data). In cross-ancestry fine-mapping results, 17 of the 45 putative causal variants were scored as "regulatory" (score < 5, with probability $p \geq 0.50$; Table S6). rs683039, located at 12 kb 5′ of *RGS17*, had the lowest RegulomeDB score (score = 1f; p = 0.93), demonstrating the largest evidence for being in a regulatory region (Figure S1). In European-ancestry fine-mapping results, six of the eight putative causal variants were scored as regulatory (score < 5, with $p \geq 0.50$; Table S7). rs2925979, located near *CMIP*, had the lowest RegulomeDB score (score = 2b; p = 0.75), demonstrating the largest evidence of being in a regulatory region.

Causal variants enriched for cardiometabolic traits

We also examined our nominated causal variants for shared genetic architecture with fine-mapping results of 2,629 unique traits from over 3,052 GWAS summary statistics obtained from the CAUSALdb database,[29] which includes UK Biobank and other cohorts. When a candidate adiponectin-causal variant was reported in more than one prior study, we meta-analyzed the p values. In total, we found 306 unique lead variant-trait combinations that are Bonferroni significant (Table S8; Figure S8). We observed that most of our nominated causal variants show prior strong associations for liver-related diseases, type 2 diabetes mellitus, hormones, body size, and body composition measurements (Figure S8).

Gene prioritization highlights genes underlying adiponectin association signals

GPScore to nominate locus-specific target genes

Variants underlying genetic association signals do not necessarily regulate the closest gene.[49–53] To assess and prioritize

Table 1. Cross-ancestry meta-analysis of adiponectin associations

						EAF	Fixed effects				Random effects (RE2)	MR-MEGA	Replication	
Lead variant	Chr	Position	Nearest gene	N	EA/NEA	(ADIPOGen/METSIM/AGEN)	p value	Beta	SE	I2	p value	Bayes factor	p value FE	p value RE2
Novel loci achieving genome-wide significance in multi-ancestry meta-analysis														
rs333947	1	110,470,764	*CSF1*	46,340	A/G	0.15/0.18/0.28	1.22E−08	−0.031	0.006	42.5	9.88E−02	33.2	4.35E−11	7.10E−11
rs596359	6	153,457,053	*RGS17*	46,408	T/C	0.43/0.45/0.26	2.43E−08	0.023	0.004	76.3	5.04E−02	36.9	9.34E−09	1.12E−08
rs10787516	10	115,813,924	*ADRB1*	46,406	T/C	0.40/0.46/0.59	1.24E−09	0.026	0.004	71.3	6.46E−02	41.2	8.10E−14	7.46E−14
rs11023332	11	14,784,110	*PDE3B*	46,367	C/G	0.43/0.44/0.35	3.27E−08	−0.022	0.004	7.1	1.10E−01	30.0	2.83E−11	4.65E−11
rs2657888	12	56,938,383	*RBMS2*	45,417	T/G	0.36/0.39/0.25	2.60E−09	0.025	0.004	15.6	8.36E−02	35.1	1.59E−04	8.01E−10
rs601339	12	123,174,743	*HCAR1*	46,388	G/A	0.15/0.17/0.49	2.33E−14	0.040	0.005	0.0	2.45E−02	55.8	3.11E−19	6.65E−19
rs222852	17	7,140,606	*PHF23*	46,404	G/A	0.49/0.38/0.37	3.83E−09	0.026	0.004	67.7	8.35E−02	38.2	7.40E−12	1.25E−11
Previously reported loci achieving genome-wide significance in multi-ancestry meta-analysis														
rs2061155	1	219,665,008	*LYPAL1-AS1*	46,406	T/C	0.40/0.37/0.37	5.34E−09	−0.024	0.004	70.5	9.03E−02	38.2	6.56E−16	1.22E−17
rs1515108	2	227,123,086	*IRS1*	46,370	T/C	0.38/0.39/0.91	2.30E−11	−0.028	0.004	89.6	1.22E−03	61.2	3.92E−15	8.18E−17
rs1108842	3	52,720,080	*PBRM1*	46,400	C/A	0.46/0.47/0.57	7.04E−16	0.033	0.004	78.6	1.08E−02	71.8	3.77E−20	6.87E−20
rs17366568	3	186,570,453	*ADIPOQ*	38,849	A/G	0.09/0.14/0.03	7.90E−99	−0.168	0.007	89.4	4.45E−12	461.5	6.66E−168	5.00E−174
rs13131633	4	89,739,479	*FAM13A*	46,349	T/C	0.49/0.45/0.65	1.85E−08	−0.023	0.004	66.8	1.03E−01	35.0	2.76E−12	2.35E−12
rs6450176	5	53,298,025	*ARL15*	46,302	A/G	0.23/0.23/0.44	1.43E−12	−0.033	0.005	69.4	2.93E−02	54.0	1.48E−18	5.34E−19
rs998584	6	43,757,896	*VEGFA*	45,226	A/C	0.48/0.50/0.56	8.19E−12	−0.033	0.005	57.5	4.52E−02	48.7	6.74E−14	1.23E−13
rs2980879	8	126,481,475	*TRIB1*	41,147	T/A	0.38/0.28/0.28	2.06E−09	0.028	0.005	0.0	8.15E−02	34.3	NA	NA
rs10886863	10	122,929,493	*WDR11-FGFR2*	38,199	T/C	0.008/0.07/0.36	1.80E−12	0.077	0.011	71.4	2.65E−02	54.0	6.92E−09	7.23E−12
rs11045172	12	20,470,221	*PDE3A*	44,409	C/A	0.19/0.23/0.79	4.03E−12	0.040	0.005	31.0	4.20E−02	48.3	5.49E−20	5.18E−20
rs10778506	12	107,143,260	*RFX4*	46,400	T/C	0.47/0.29/0.67	1.60E−08	0.024	0.004	55.6	1.02E−01	33.7	2.02E−03	8.69E−12
rs7978610	12	124,468,572	*ZNF664*	44,745	C/G	0.39/0.27/0.08	7.94E−16	0.037	0.005	91.6	1.87E−04	86.0	1.08E−27	1.33E−32
rs2925979	16	81,534,790	*CMIP*	46,408	T/C	0.28/0.31/0.41	5.59E−28	−0.049	0.004	71.1	6.88E−04	124.5	1.10E−09	2.66E−42
rs12051272	16	82,663,288	*CDH13*	32,655	T/G	0.009/0.11/0.29	3.89E−213	−0.358	0.011	94.2	1.41E−24	1002.5	1.37E−232	1.65E−237
rs731839	19	33,899,065	*PEPD*	46,229	A/G	0.33/0.34/0.46	3.28E−21	0.042	0.004	75.1	2.53E−03	94.7	3.41E−36	1.91E−39

A locus ≥500 kb from a previously reported adiponectin-associated variant achieving genome-wide significance ($p < 5E{-}08$; GWAS catalog, January 2023) is considered to be previously unreported.
Lead variant at each locus attaining genome-wide significance ($p < 5 \times 10{-}8$) in the cross-ancestry meta-analysis (ADIPOGen, AGEN, METSIM).

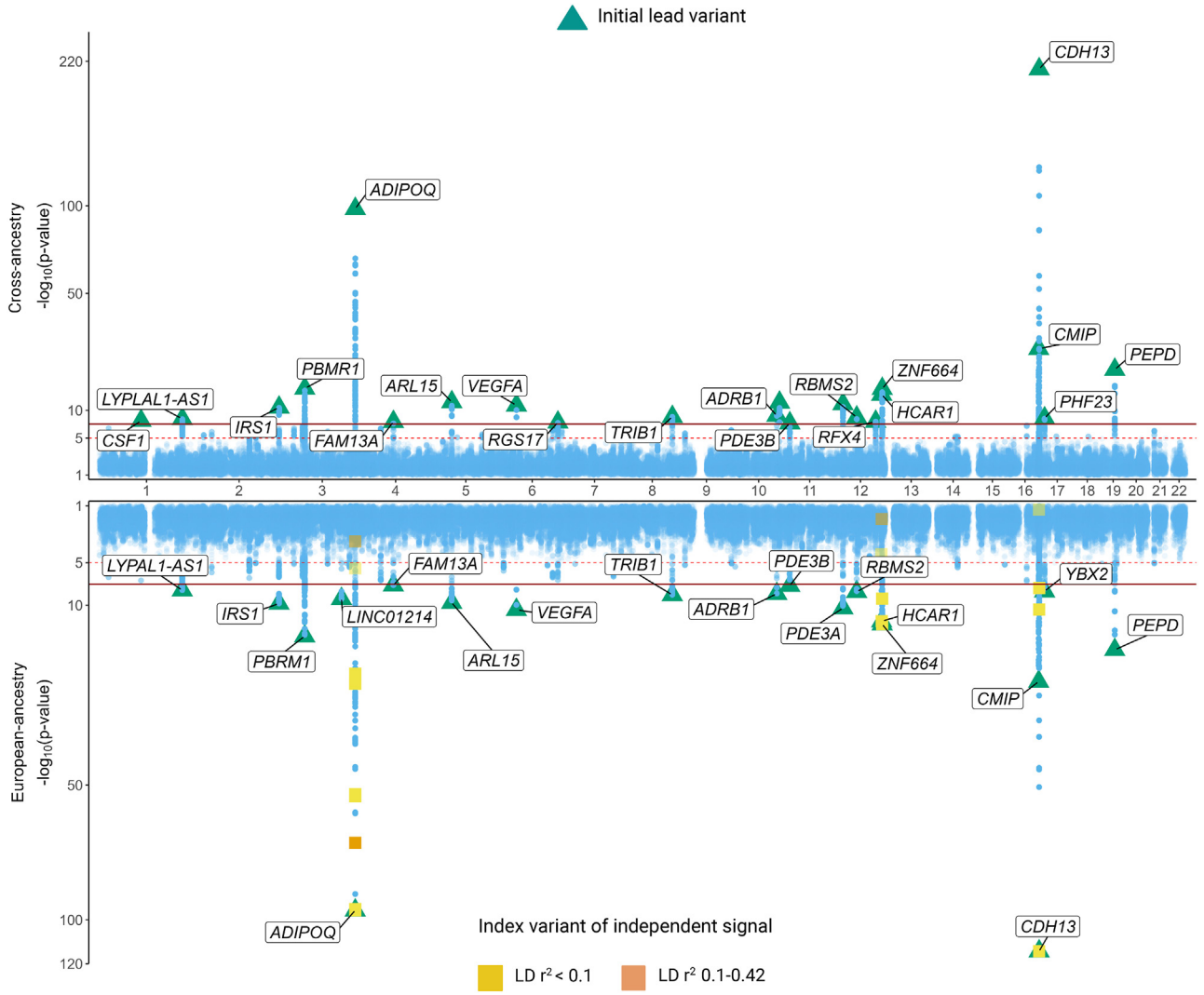

Figure 1. Miami plot of the multi-ancestry (top) and European-ancestry (bottom) genome-wide meta-analysis results for adiponectin

The y-axis represents $-\log_{10}$(P) value from the fixed-effects analyses. Each blue dot represents a variant tested in the meta-analysis. The transcript closest to the lead variant (triangles) at each locus is listed in rectangle boxes. Index variants from the additional distinct association signals identified in the European-ancestry meta-analyses are denoted by squares and colored based on the linkage disequilibrium with the lead variant at that locus (orange: $0.10<r^2<0.42$; yellow $r_2<0.10$).

target genes underlying adiponectin-associated signals, we developed a combinatorial likelihood scoring formalism (GPScore) based upon measures derived from 11 gene prioritization strategies (Tables S9–S30), along with the physical distance to the TSSs (Figure 2). We integrated multiple lines of evidence into the score by using four terms: p_G (combined p value), S_G (combined scaled scores), C_S (proportion of support), and TSS_d (distance from TSS of the gene to the lead GWAS variant). The most likely target gene(s) were selected based on the highest locus-specific GPScore within the 3-Mb window. For the four regions with overlapping windows (12q24.31 near *HCAR1* and *ZNF664* and 16q23 near *CMIP* and *CDH13*), the flanking size of 1.5 Mb is reduced to 1 Mb to limit the window overlap.

In cross-ancestry analysis, we prioritized a total of 30 genes with high relative locus-specific GPScore values across 22 locus windows(Tables 3 and S31; Figure 3). Out of 22 regions, 15 had one prioritized gene, six had two prioritized genes (*PBRM1*; OMIM: 606083 and *GNL3*; OMIM: 608011 at 3p21.1, *ADIPOQ* and *RFC4*; OMIM: 102577 at 3q27.3, *NAP1L5*; OMIM: 612203 and *FAM13A*; OMIM: 613299 at 4q22.1, *FDGFR2* and *WDR11* OMIM: 606417 at 10q26.12, *CTDNEP1*; OMIM: 610684 and *ELP5*; OMIM: 615019 at chr17p13.1, and *PEPD*; OMIM: 613230, and *CEBPG*; OMIM: 138972 at 17p13.1), and one region had three prioritized genes (*CCDC92*, *DNAH10OS*, and *ZNF664* at 12q24.31) (Table 3; Figure 3). GPScore prioritized well-known adiponectin target genes concerning various cardiovascular/cardiometabolic diseases, including *IRS1*, *ADIPOQ*, *PDE3A*, *CCDC92*, and *CDH13*.[54–58] GPScore also prioritized target genes for previously unreported loci that have been shown to play key

Table 2. Meta-analysis of adiponectin associations in European-ancestry population

						EAF	Fixed effects					Random effects (RE2)	
Lead variant	Chr	hg19 position	Nearest gene	N	EA/NEA	(ADIPOGen/METSIM)	p value	Beta	SE	I2	Q-value	p value	Heterogeneity
Novel loci for any adiposity trait achieving genome-wide significance in European-ancestry meta-analysis													
rs7617025	3	150,055,958	*LINC01214*	38,578	A/G	0.09/0.07	7.47E−10	−0.045	0.007	0.0	0.6	1.10E−09	0.0
rs10787516	10	115,813,924	*ADRB1*	38,579	C/T	0.40/0.46	3.33E−09	0.026	0.004	85.6	6.9	2.47E−09	1.3
rs11023332	11	14,784,110	*PDE3B*	38,540	C/G	0.43/0.44	3.24E−08	−0.023	0.004	37.8	1.6	4.08E−08	0.00
rs2657888	12	56,938,383	*RBMS2*	38,562	G/T	0.36/0.39	5.92E−09	−0.025	0.004	57.5	2.4	8.44E−09	0.0
rs601339	12	123,174,743	*HCAR1*	38,561	G/A	0.15/0.17	4.88E−13	0.039	0.005	0.0	0.2	8.38E−13	0.0
rs17805277	17	7,201,753	*YBX2*	35,526	G/T	0.11/0.13	6.94E−09	0.042	0.007	0.0	0.7	9.86E−09	0.0
Previously reported loci achieving genome-wide significance in European-ancestry meta-analysis													
rs2061155	1	219,665,008	*LYPLAL1-AS1*	38,579	C/T	0.40/0.37	9.10E−09	−0.025	0.004	84.8	6.6	8.00E−09	0.9
rs2943657	2	227,123,439	*IRS1*	38,543	C/T	0.38/0.39	1.71E−10	−0.028	0.004	94.2	17.4	1.93E−12	9.8
rs1108842	3	52,720,080	*PBRM1/STAB1*	38,574	C/A	0.46/0.47	2.00E−15	0.033	0.004	88.7	8.9	1.00E−15	2.6
rs16861209	3	186,563,114	*ADIPOQ*	38,435	A/C	0.01/0.03	1.30E−96	0.204	0.010	96.5	28.3	3.73E−100	19.3
rs13131633	4	89,739,479	*FAM13A*	38,524	C/T	0.49/0.45	3.59E−08	−0.023	0.004	83.2	5.9	3.53E−08	0.5
rs6450176	5	53,298,025	*ARL15*	38,475	A/G	0.23/0.23	2.23E−10	−0.032	0.005	81.1	5.3	3.12E−10	0.2
rs998584	6	43,757,896	*VEGFA*	37,403	A/C	0.48/0.50	2.36E−11	−0.033	0.005	77.9	4.5	3.76E−11	0.0
rs2980879	8	126,481,475	*TRIB1*	33,320	A/T	0.38/0.28	2.36E−09	0.029	0.005	0.0	0.4	3.44E−09	0.0
rs11045172	12	20,470,221	*PDE3A*	36,583	A/C	0.19/0.23	3.97E−11	0.040	0.006	65.3	2.9	6.30E−11	0.0
rs7978610	12	124,468,572	*ZNF664*	36,945	C/G	0.39/0.27	1.66E−13	0.035	0.005	89.8	9.8	5.40E−14	3.4
rs2925979	16	81,534,790	*CMIP*	38,583	C/T	0.28/0.31	5.72E−24	0.047	0.005	78.1	4.6	1.32E−23	0.0
rs12051272	16	82,663,288	*CDH13*	24,829	G/T	0.01/0.11	8.04E−115	−0.331	0.015	96.1	25.4	4.30E−118	18.3
rs731839	19	33,899,065	*PEPD*	38,402	A/G	0.33/0.34	8.69E−18	0.040	0.005	79.6	4.9	1.73E−17	0.0

Novel locus is ≥500 kb from previously reported adiponectin-associated variant achieving genome-wide significance ($p < 5E{-}08$; GWAS catalog, January 2023).
List of all lead variants achieving genome-wide significance ($p < 5 \times 10{-}8$) in the meta-analysis of adiponectin associations in the European population (ADIPOGen and METSIM).

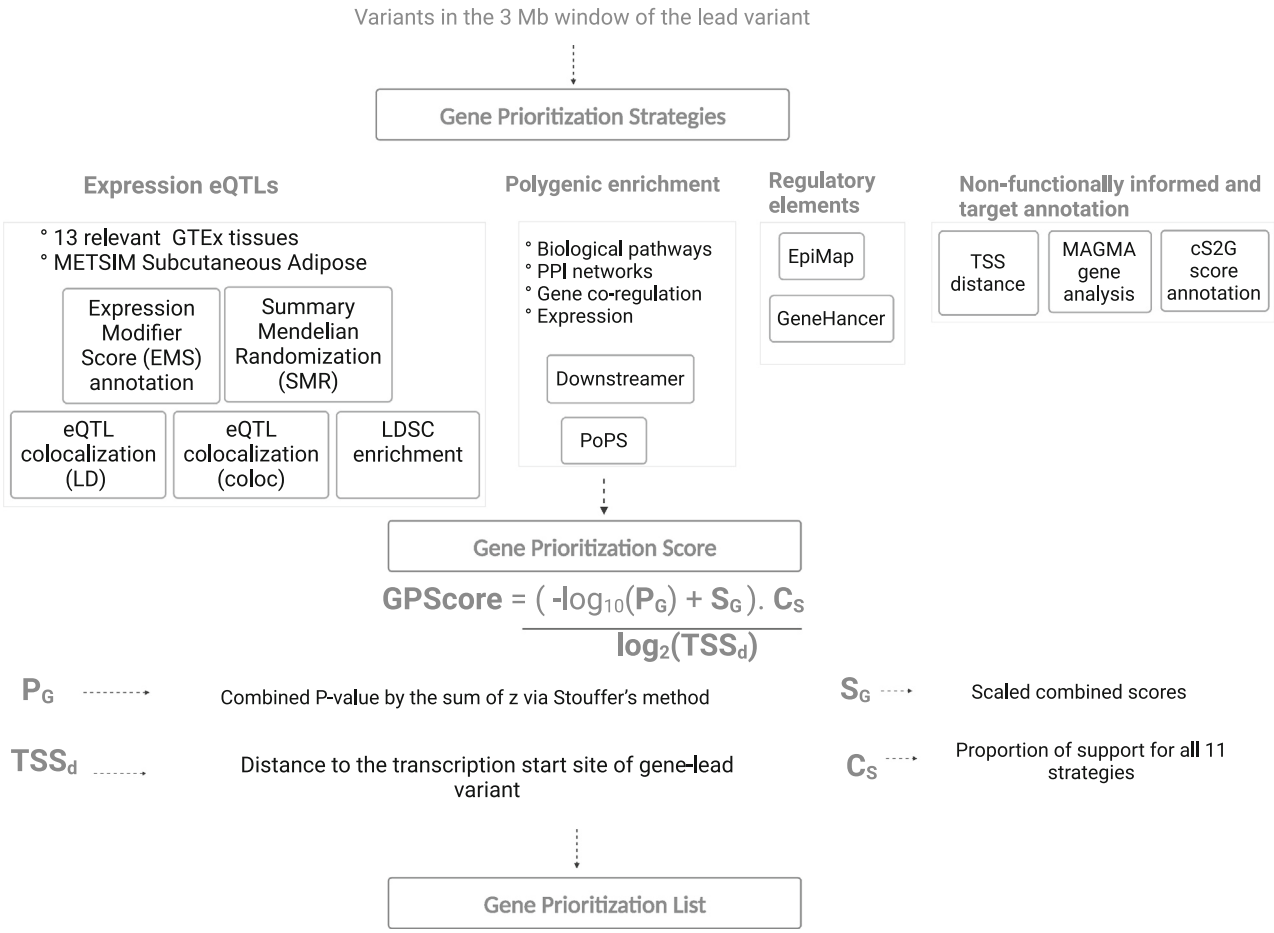

Figure 2. Schematic overview of gene prioritization score construction for finding target genes of adiponectin
Flow diagram illustrating various gene prioritization strategies using multiple data sources: expression QTLs, pathways and networks, regulatory elements, and non-functionally informed methods. The gene prioritization score incorporates all this evidence using four terms: P_G, S_G, C_S, and TSS_d (distance to the transcription start site). We prioritize locus-specific target genes using the gene prioritization score, with higher values indicating stronger support across approaches.

roles in adipose-related metabolic functions (e.g., *CSF1*, *RGS17*, *ADRB1*, and *CYP2R1*).[59–62]

Gene prioritization results using variants from the European-ancestry analysis yielded similar results to the cross-ancestry prioritization (Table S32). At the 18 loci shared between European- and cross-ancestry analyses, 13 loci yielded the same set of prioritized genes. At four of the shared loci, the European-ancestry GPScore prioritized additional target genes (Table S32). At the chr17p13.1 locus shared between the European- and cross-ancestry results, GPScore prioritized a different target gene in the European-ancestry analysis (*ACAP1*; OMIM: 607763) than in the cross-ancestry analysis (*CTDNEP1* and *ELP5*). Differences in GPScore prioritization between the two sets of analyses is likely explained by differences in effect sizes and allele frequencies used as input to the gene prioritization strategies.

To see which of the GPScore terms received the most weight in the score calculation, we quantified each term's contribution to the GPScore (Figures 4A and S9) by fitting a multiple regression model and averaging over orderings proposed by Lindeman et al. and implemented in the *realimpo* package.[63] Across the 22 cross-ancestry regions tested, the average contributions (on a scale of 0–1) were $S_G = 0.133$, $C_S = 0.199$, $TSS_d = 0.255$, and $p_G = 0.411$. The 2q36.3 window where *IRS1* is prioritized has the lowest TSS_d contribution since the transcription start site for *IRS1* is 541,389 bp away from the lead adiponectin GWAS variant but has the strongest support for being the effector gene (Table S31). The 3p21.1 window has the highest TSS_d contribution since both the prioritized genes *PBMR1* and *GNL3* are close to the lead variant (Figure 4D). The variants in 5q11.2,6p21.1 and 8q24.13 windows have the lowest contribution of C_S (proportion of support) due to a lack of support from many of the gene prioritization strategies (Figure 4A). The p_G (combined p value) has an average contribution of 0.411 across all the windows. Regarding the gene prioritization strategies, all prioritized genes have MAGMA p value $<5 \times 10^{-8}$, higher PoPS scores, and cS2G annotations while supporting the majority of other strategies (Figure S9). Because several prioritization strategies rely on a reference panel

Table 3. Adiponectin cross-ancestry meta-analysis prioritized target gene list

Lead variant	Chr: Position(hg19)	Prioritized gene	TSS to lead variant	Priority score
rs333947	1:110470764	*CSF1*	17900	1.3351
rs2061155	1:219665008	*LYPLAL1*	317822	0.2503
rs1515108	2:227123086	*IRS1*	541389	0.9413
rs1108842	3:52720080	*PBRM1*	147	3.7674
rs1108842	3:52720080	*GNL3*	4908	2.5499
rs17366568	3:186570453	*ADIPOQ*	9990	1.1682
rs17366568	3:186570453	*RFC4*	45606	0.8853
rs13131633	4:89739479	*NAP1L5*	120093	0.5508
rs13131633	4:89739479	*FAM13A*	293070	0.4818
rs6450176	5:53298025	*FST*	521786	0.3813
rs998584	6:43757896	*VEGFA*	19975	0.2982
rs596359	6:153457053	*RGS17*	4669	1.6313
rs2980879	8:126481475	*TRIB1*	38912	0.3179
rs10787516	10:115813924	*ADRB1*	10118	0.3602
rs10886863	10:122929493	*FGFR2*	428479	0.3052
rs10886863	10:122929493	*WDR11*	318806	0.2006
rs11023332	11:14784110	*CYP2R1*	129688	0.5779
rs11045172	12:20470221	*PDE3A*	51958	1.9119
rs2657888	12:56938383	*RBMS2*	22670	0.5667
rs10778506	12:107143260	*RIC8B*	25113	0.4618
rs601339	12:123174743	*HCAR2*	13147	0.9471
rs7978610	12:124468572	*CCDC92*	11194	3.0608
rs7978610	12:124468572	*DNAH10OS*	49041	2.0406
rs7978610	12:124468572	*ZNF664*	12180	2.0127
rs2925979	16:81534790	*CMIP*	56015	0.8602
rs12051272	16:82663288	*CDH13*	2880	3.3914
rs222852	17:7140606	*CTDNEP1*	15204	1.5380
rs222852	17:7140606	*ELP5*	14129	1.3088
rs731839	19:33899065	*PEPD*	113635	0.5830
rs731839	19:33899065	*CEBPG*	34829	0.5403

Prioritization of 30 likely target/effector genes by using locus-specific gene priority score constructed from 11 gene prioritization strategies along with TSS distance.

for LD calculation, we repeated GPScore using only the METSIM cohort summary statistics; the top prioritized genes for the common windows remain the same (Table S33).

GPScore to nominate target genes of other traits

We validated the GPScore using three traits from the FinnGen consortium,[64] specifically focusing on idiopathic pulmonary fibrosis (target gene *TERT*; OMIM: 187270), monogenic diabetes (target gene *RFX6*; OMIM: 612659), and autoimmune hypothyroidism (target gene *TG*; OMIM: 188450). The GPScore was formulated by integrating multiple gene prioritization strategies and was effective in identifying known target genes for these traits, as detailed in Tables S34, S35, and S36. Additional details are provided in the supplemental information.

Evaluating disease associations and functional interactions

Disease enrichment analysis

We evaluated the association of cross-ancestry prioritized genes with disease phenotypes using gene-disease enrichment analysis.[44,45] We found a strong enrichment (adjusted $p < 0.01$) of DisGeNET terms related to cardiometabolic traits and diseases, including waist-hip ratio,

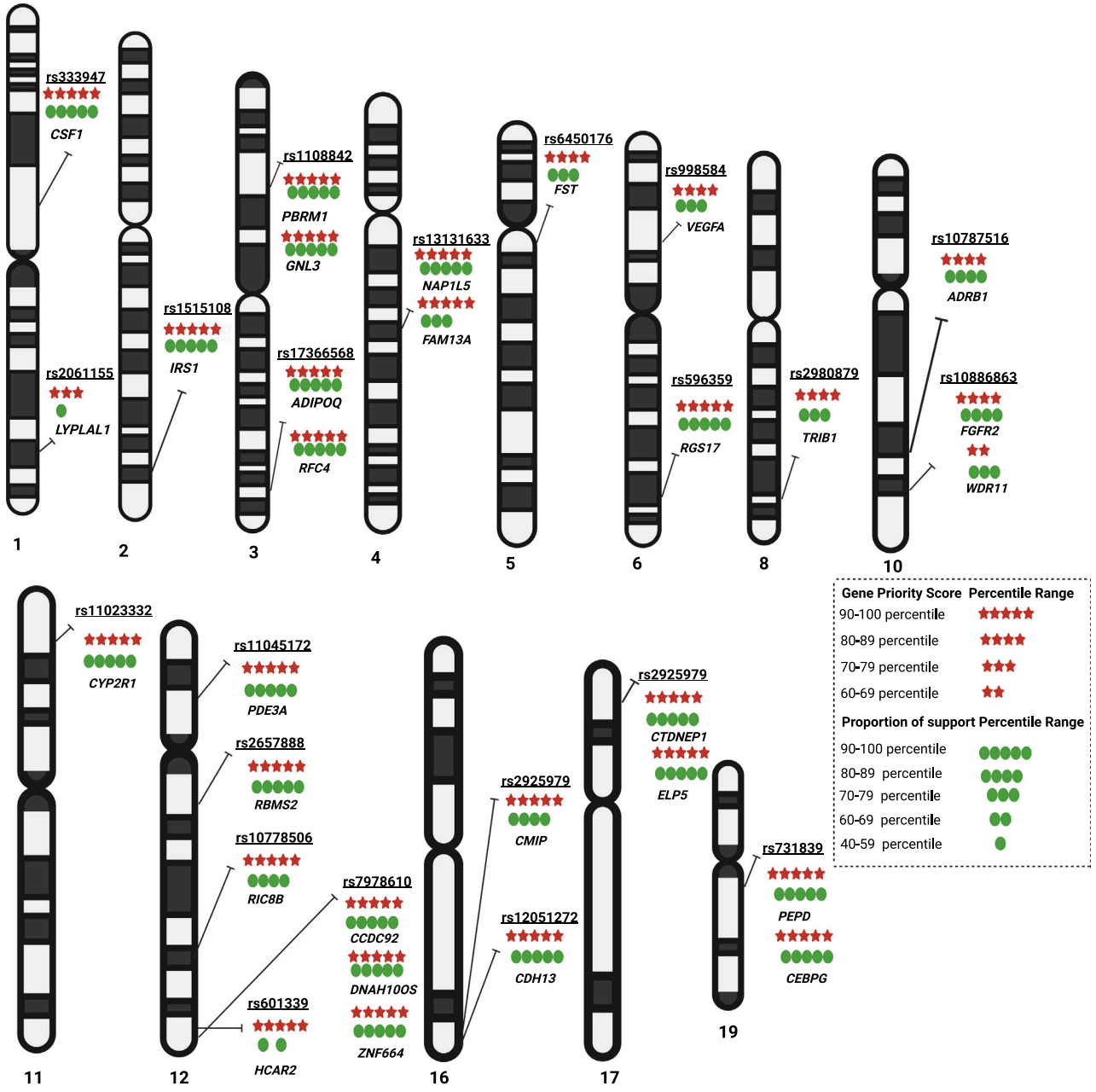

Figure 3. Adiponectin locus-specific prioritized genes and strength

A chromosome ideogram depicts the location and strength of GPscore values, C_s (proportion of support) of each prioritized gene identified in an adiponectin multi-ancestry meta-analysis. Red stars highlight the strength of the GPscore measured in percentile, whereas green circles highlight the proportion of support from the 11 prioritization approaches. Some locations have multiple prioritized genes with relatively similar scores.

arteriosclerosis obliterans, non-alcoholic fatty liver disease, BMI, coronary artery disease, hypoadiponectinemia, and high-density lipoprotein measurement (Figure 5A; Tables S34 and S35). Other highly enriched terms are related to cancer outcomes, including thymoma, endometrial neoplasms, endometrial adenocarcinoma, giant cell tumors, noninfiltrating intraductal carcinoma, and non-hereditary clear cell renal cell carcinoma. These findings support recent epidemiological evidence that links adiponectin to cancer.[65,66]

Functional association network

For the cross-ancestry meta-analysis results, we constructed an interactive functional association network illustrating the relationships among the connected genes, prioritized genes, and associated pathways (Figures 5 and S10; Tables S36–S39). In Figure 5, we display the network results where we use the default of adding 20 "related" genes and pathways into the network. With the default network size, 76.6% of our prioritized genes (23 out of 30) were incorporated into functional

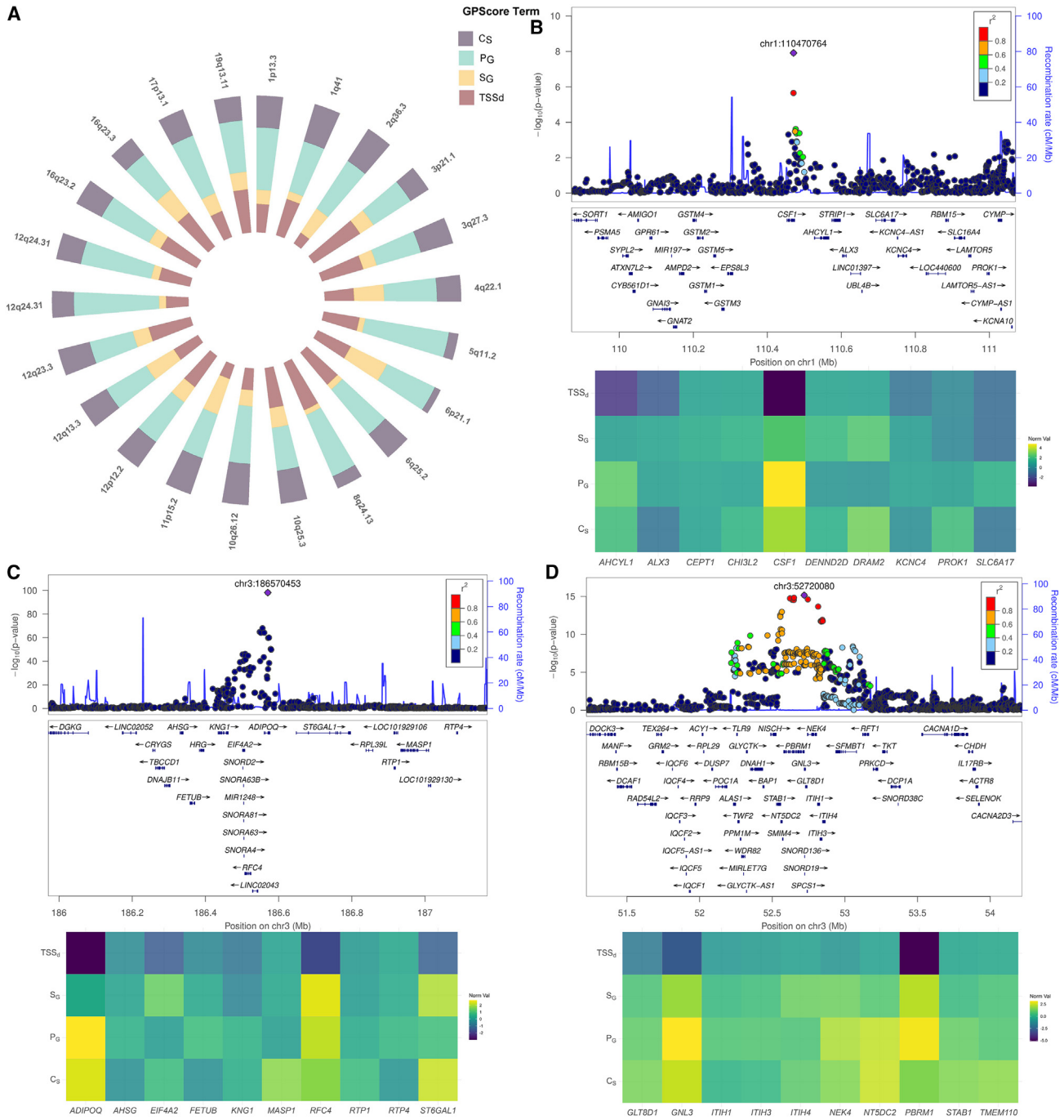

Figure 4. The relative contribution of terms from the Gene Priority Score and illustrative biological examples

(A) Relative importance of four terms: P_G, S_G, C_S, and TSS_d for the gene priority score construction across 22 associated regions in multi-ancestry analysis.

(B–D) Top: Locus zoom plots of multi-ancestry summary statistics, colored by LD with the lead variant. The color of the heatmap represents enrichment for the GPScore term. The top prioritized genes at each exemplary locus are *CSF1* (B), *ADIPOQ* and *RFC4* (C), *GNL3* and *PBRM1* (D).

association networks, with most having multiple connected genes (Figure 5B). A total of 10 pathways were represented in the network, with many genes heavily involved in the adipocytokine signaling pathway, integrins in angiogenesis, leptin pathway, and type 2 diabetes.

Discussion

Adiponectin is an insulin-sensitizing and anti-inflammatory hormone secreted by adipocytes whose signaling is involved in several metabolic processes crucial to type 2 diabetes, neurodegeneration, and cardiovascular disease.

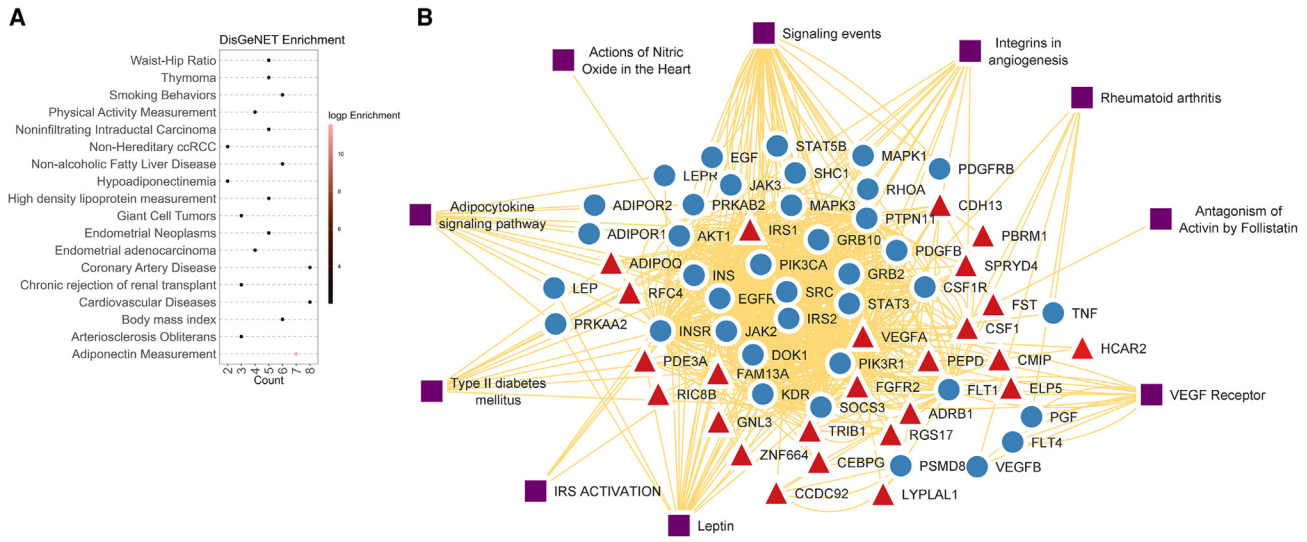

Figure 5. Disease enrichment and functional interaction network of adiponectin multi-ancestry prioritized genes
(A) Select results from the disease enrichment analysis (DisGeNET, enrichr) using the multi-ancestry prioritized genes list. DisGeNET terms related to cardiovascular/cardiometabolic traits show strong enrichment (adjusted $p < 0.01$).
(B) An interactive functional association network, illustrating the relationships among the connected genes, prioritized genes, and underlying associated pathways constructed using GeneMANIA. A total of 10 pathways were represented in the network (purple squares). A complete network is shown in Figure S10.

In this study, we conducted the largest cross-ancestry adiponectin GWAS meta-analysis to date, in up to 46,434 individuals from the METSIM cohort and the ADIPOGen and AGEN consortiums. We identified 22 loci associated with adiponectin ($p < 5 \times 10^{-8}$), including 15 known and seven additional loci. European-ancestry results revealed 14 additional secondary signals at the *ADIPOQ*, *CDH13*, *HCAR1*, and *ZNF664* loci. Most of the lead variants showed associations with other complex traits/diseases, suggesting pleiotropy. We narrowed the list of putative causal variants to 46 (PP > 0.9), 17 of which demonstrated moderate to strong regulatory evidence. Our nominated causal variants also showed potential pleiotropy for other complex cardiometabolic traits, such as liver-related diseases, type 2 diabetes, hormones, body size, and body compositional measurements.

Variants underlying genetic association signals may not necessarily regulate the closest gene[49-53] and may affect protein levels thousands or even millions of base pairs away.[67] Based on prior estimates,[68] the 3-Mb fine-mapping region (±1.5 Mb around the index variant) should roughly capture more than 99% of such regulatory activity. Multiple methods currently exist to prioritize target, or effector, genes underlying GWAS signals, primarily from gene eQTL data,[10] regulatory genomic activity,[11] and protein-protein interaction networks and pathway databases.[12] Two common challenges of existing gene prioritization approaches are (1) inadequate customizability to represent the data which is disease/tissue relevant, and (2) conflicting findings from various approaches due to differences in assumptions, methodology, and representation models, resulting in the selection of methods/results in an *ad hoc* or *post hoc* manner. To address these limitations, we developed combinatorial likelihood scoring formalism, GPScore, based upon measures derived from 11 gene prioritization strategies, along with the physical distance to the TSSs. GPScore integrates multiple lines of evidence into a score that can be customizable to include weighting factors to prioritize signals from a particular tissue and can be broadly applicable to other complex traits that do not have much training data. By utilizing GPScore, we prioritize the 30 most probable target/effector genes for adiponectin in the cross-ancestry analysis.

The prioritized gene list includes several well-known causal genes related to serum adiponectin levels. This list includes *ADIPOQ*, which is responsible for encoding the adiponectin protein, and *CDH13*, which encodes an adiponectin receptor protein.[56] Insulin receptor substrate-1 (*IRS1*) is a substrate of the insulin receptor tyrosine kinase, and it is central to inducing insulin actions, including binding and activating phosphatidylinositol 3-kinase (PI3K) and increasing glucose transport.[69] Acute knockdown in adipocytes was shown to result in increased Adipoq mRNA expression but reduced adiponectin secretion.[70] The treatment of myoblast cell line (C2C12) with adiponectin was also shown to enhance the ability of insulin to stimulate *IRS-1* tyrosine phosphorylation and Akt phosphorylation.[55] *CCDC92* has been shown to be important in insulin resistance and influencing adipocyte differentiation,[71] and knockdown of *CCDC92* in mice was shown to reduce obesity and insulin resistance.[72] We also used GPScore to prioritize target genes among our additional loci from our cross-ancestry meta-analysis, including several for which the biological mechanisms underlying the association with adiponectin may be unclear. The *CSF-1* gene, which was prioritized at 1p13.3, has been shown to have

therapeutic potential in tissue repair[73] due to its involvement in macrophage homeostasis and inflammation via the *CSF-1* receptor.[74] There is also some supportive evidence that *CSF-1/CSF-1R* signaling is essential in the pathology of diabetes.[75] Due to its essential role in G protein signaling, *RGS17* is considered a potential therapeutic target for lung and prostate cancers[76]; however, individuals with type 2 diabetes have been shown to have higher levels of *RGS17* auto antibodies than individuals without type 2 diabetes, and expression levels of *RGS17* are significantly upregulated in adipose tissue during periods of weight loss.[77] *ADRB1*, which encodes the adrenergic beta-1 receptor, was prioritized at 10q25.3. While ADRB1 is most known for the functional role it plays in cardiomyocyte function,[78,79] visceral adiponectin release was shown to be triggered by cyclic AMP (cAMP) via signaling pathways involving adrenergic beta receptors in mice. The CYP2R1 protein, a receptor for vitamin D 25-hydroxylase in the liver,[80] plays a crucial role in non-alcoholic fatty liver disease.[81] Epidemiological studies have also demonstrated associations between serum vitamin D and adiponectin levels. While there is less existing evidence to support the mechanism(s) between some of the prioritized genes and adiponectin levels (e.g., *TRIB1*, *RBMS2*), a further experimental examination into the prioritized genes is warranted.

Our functional profiling of prioritized genes with human disease phenotypes revealed the enrichment of terms related to cardiovascular diseases, coronary artery disease, and other cardiometabolic traits. Interestingly, many genes also showed enrichment related to cancer etiopathogenesis, and recent evidence has shown adiponectin's antiangiogenic and tumor growth-limiting properties of adiponectin.[65] Our functional association network analysis also helped illustrate the complex interactions of prioritized genes, their functionally connected genes, and their underlying pathways. We observed the key underlying pathways centered on insulin signaling (through *IRS1*, *IRS2*, *INS*, *INSR*) and adiponectin signaling (thorough *ADIPOR1*, *ADIPOR2*) suggesting potential crosstalk and an essential role in regulating energy balance in the body, inflammation, coagulation, fibrinolysis, insulin resistance, and diabetes. The observed enrichment is in line with previous Mendelian randomization studies between adiponectin-associated variants and several cardiometabolic and diabetic outcomes.[82–85]

There are several caveats to our current GPScore gene prioritization approach that should be considered. First, while we were able to utilize our approach in both single- and cross-ancestry summary data, our cross-ancestry analysis is still primarily European (83.14%) and includes only one other ancestry population (East Asian ancestry); thus, more diverse studies are needed to determine if our approach is less robust when including data with additional heterogeneity. Because our data were largely from European-ancestry populations, we used data from 10,197 Finnish METSIM participants as the reference for LD calculations for our fine-mapping and gene prioritization strategies. We acknowledge, however, that this is likely not the most appropriate panel for LD calculation in our cross-ancestry population. We plan to expand our work by utilizing a larger, more diverse ancestry LD reference panel. However, the flexibility of our approach allows researchers to determine the most appropriate LD panel for their study population. The GPScore prioritization procedure depends on the quality and availability of disease/cell-relevant data, the accuracy of the strategy used, and the annotation quality of variants and genes. As additional data become available, they could easily be incorporated into our GPScore approach. It is also possible that transforming variant/position-level scores into gene-level scores may result in a loss of information; however, this information is still retained in the initial prioritization approaches and could still be considered. Although some of the underlying data are used in more than one of the approaches (e.g., expression data), the results for each approach can differ due to variations in assumptions, methodologies, hypotheses tested, and representation models used by the tools. Last, while it is beneficial to rank genes in a locus-specific manner, the strength of GPScore does not implicate causality for a complex trait or disease, nor is it comparable across locus windows. We acknowledge that the absence of a complete set of causal and non-causal or true set genes for adiponectin presents challenges in the validation process. Further analysis is necessary to thoroughly assess the applicability of GPScore to other complex traits.

In conclusion, we discovered 15 known and seven previously unreported genomic loci associated with adiponectin through cross-ancestry genome-wide meta-analysis. The 45 putative causal variants identified through fine-mapping showed potential pleiotropy for cardiovascular/metabolic traits. In addition, we provide a customizable gene prioritization method, GPScore, that integrates multiple lines of evidence, thus increasing the likelihood of identifying the true target gene underlying a GWAS association signal. Our prioritized genes and underlying pathways yield new insights into the genetic architecture of adiponectin. Future research should include phenotyping of adiponectin in large-scale, diverse biobanks and cohorts, thus increasing sample size and ancestral diversity for robust prediction of target genes.

Data and code availability

The summary statistics generated from this study are available from the GWAS catalog, accession numbers GCST90293085 and GCST90293086. The code to reproduce the analyses and figures of this paper is available as Jupyter Notebooks at https://github.com/vsarsani/GPScore.

Supplemental information

Supplemental information can be found online at https://doi.org/10.1016/j.xhgg.2023.100252.

Acknowledgments

We thank the individuals in the METSIM cohort for their continued study participation. We want to acknowledge the participants and investigators of the FinnGen study.

Declaration of interests

The authors declare no competing interests.

Received: June 29, 2023
Accepted: October 16, 2023

Web resources

Online Mendelian Inheritance in Man (OMIM): https://www.ncbi.nlm.nih.gov/omim/. CMDKP: www.cmdkp.org. RegulomeDB: https://regulomedb.org/. CAUSALdb: http://www.mulinlab.org/causaldb/. EMS annotation: https://www.finucanelab.org/data. Epimap: https://personal.broadinstitute.org/cboix/epimap/links/pergroup/. GeneHancer and cS2G: https://zenodo.org/record/7754032#.ZEP6AvzMIQ8. FinnGen database: (https://www.finngen.fi/).

References

1. Achari, A.E., and Jain, S.K. (2017). Adiponectin, a Therapeutic Target for Obesity, Diabetes, and Endothelial Dysfunction. Int. J. Mol. Sci. *18*.
2. Tilg, H., and Moschen, A.R. (2006). Adipocytokines: mediators linking adipose tissue, inflammation and immunity. Nat. Rev. Immunol. *6*, 772–783.
3. Li, S., Shin, H.J., Ding, E.L., and van Dam, R.M. (2009). Adiponectin levels and risk of type 2 diabetes: a systematic review and meta-analysis. JAMA *302*, 179–188.
4. Dastani, Z., Hivert, M.F., O'Leary, D.H., Perry, J.R.B., Yuan, X., Scott, R.A., Henneman, P., Heid, I.M., Kizer, J.R., Lyytikäinen, L.P., et al. (2012). Novel loci for adiponectin levels and their influence on type 2 diabetes and metabolic traits: a multi-ethnic meta-analysis of 45,891 individuals. PLoS Genet. *8*, e1002607.
5. Wu, Y., Gao, H., Li, H., Tabara, Y., Nakatochi, M., Chiu, Y.F., Park, E.J., Wen, W., Adair, L.S., Borja, J.B., et al. (2014). A meta-analysis of genome-wide association studies for adiponectin levels in East Asians identifies a novel locus near WDR11-FGFR2. Hum. Mol. Genet. *23*, 1108–1119.
6. Spracklen, C.N., Iyengar, A.K., Vadlamudi, S., Raulerson, C.K., Jackson, A.U., Brotman, S.M., Wu, Y., Cannon, M.E., Davis, J.P., Crain, A.T., et al. (2020). Adiponectin GWAS loci harboring extensive allelic heterogeneity exhibit distinct molecular consequences. PLoS Genet. *16*, e1009019.
7. Spracklen, C.N., Karaderi, T., Yaghootkar, H., Schurmann, C., Fine, R.S., Kutalik, Z., Preuss, M.H., Lu, Y., Wittemans, L.B.L., Adair, L.S., et al. (2019). Exome-Derived Adiponectin-Associated Variants Implicate Obesity and Lipid Biology. Am. J. Hum. Genet. *105*, 670–671.
8. Mahajan, A., Spracklen, C.N., Zhang, W., Ng, M.C.Y., Petty, L.E., Kitajima, H., Yu, G.Z., Rüeger, S., Speidel, L., Kim, Y.J., et al. (2022). Multi-ancestry genetic study of type 2 diabetes highlights the power of diverse populations for discovery and translation. Nat. Genet. *54*, 560–572.
9. Fisman, E.Z., and Tenenbaum, A. (2014). Adiponectin: a manifold therapeutic target for metabolic syndrome, diabetes, and coronary disease? Cardiovasc. Diabetol. *13*, 103.
10. Aguet, F., Anand, S., Ardlie, K.G., Gabriel, S., Getz, G.A., Graubert, A., Hadley, K., Handsaker, R.E., Huang, K.H., Kashin, S., et al. (2020). The GTEx Consortium atlas of genetic regulatory effects across human tissues. Science *369*, 1318–1330.
11. Boix, C.A., James, B.T., Park, Y.P., Meuleman, W., and Kellis, M. (2021). Regulatory genomic circuitry of human disease loci by integrative epigenomics. Nature *590*, 300–307.
12. Szklarczyk, D., Gable, A.L., Lyon, D., Junge, A., Wyder, S., Huerta-Cepas, J., Simonovic, M., Doncheva, N.T., Morris, J.H., Bork, P., et al. (2019). STRING v11: protein-protein association networks with increased coverage, supporting functional discovery in genome-wide experimental datasets. Nucleic Acids Res. *47*, D607–D613.
13. Aragam, K.G., Jiang, T., Goel, A., Kanoni, S., Wolford, B.N., Weeks, E.M., Wang, M., Hindy, G., Zhou, W., , et al.Atri, D.S., von Scheidt, M. (2022). Discovery and systematic characterization of risk variants and genes for coronary artery disease in over a million participants. Nat. Genet. *54*, 1803–1815.
14. Schwartzentruber, J., Cooper, S., Liu, J.Z., Barrio-Hernandez, I., Bello, E., Kumasaka, N., Young, A.M.H., Franklin, R.J.M., Johnson, T., Estrada, K., et al. (2021). Genome-wide meta-analysis, fine-mapping and integrative prioritization implicate new Alzheimer's disease risk genes. Nat. Genet. *53*, 392–402.
15. Laakso, M., Kuusisto, J., Stančáková, A., Kuulasmaa, T., Pajukanta, P., Lusis, A.J., Collins, F.S., Mohlke, K.L., and Boehnke, M. (2017). The Metabolic Syndrome in Men study: a resource for studies of metabolic and cardiovascular diseases. J. Lipid Res. *58*, 481–493.
16. Han, B., and Eskin, E. (2011). Random-effects model aimed at discovering associations in meta-analysis of genome-wide association studies. Am. J. Hum. Genet. *88*, 586–598.
17. Mägi, R., Horikoshi, M., Sofer, T., Mahajan, A., Kitajima, H., Franceschini, N., McCarthy, M.I., COGENT-Kidney Consortium T2D-GENES Consortium, and Morris, A.P. (2017). Trans-ethnic meta-regression of genome-wide association studies accounting for ancestry increases power for discovery and improves fine-mapping resolution. Hum. Mol. Genet. *26*, 3639–3650.
18. Fishilevich, S., Nudel, R., Rappaport, N., Hadar, R., Plaschkes, I., Iny Stein, T., Rosen, N., Kohn, A., Twik, M., Safran, M., et al. (2017). GeneHancer: Genome-wide Integration of Enhancers and Target Genes in GeneCards. Database (Oxford) *2017*, bax028.
19. Yang, J., Ferreira, T., Morris, A.P., Medland, S.E., Genetic Investigation of ANthropometric Traits GIANT Consortium; and DIAbetes Genetics Replication And Meta-analysis DIAGRAM Consortium, Madden, P.A.F., Heath, A.C., Martin, N.G., Montgomery, G.W., et al. (2012). Conditional and joint multiple-SNP analysis of GWAS summary statistics identifies additional variants influencing complex traits. Nat. Genet. *44*, 369–375. S1-S3.
20. Ferkingstad, E., Sulem, P., Atlason, B.A., Sveinbjornsson, G., Magnusson, M.I., Styrmisdottir, E.L., Gunnarsdottir, K., Helgason, A., Oddsson, A., Halldorsson, B.V., et al. (2021). Large-scale integration of the plasma proteome with genetics and disease. Nat. Genet. *53*, 1712–1721.
21. Benner, C., Spencer, C.C.A., Havulinna, A.S., Salomaa, V., Ripatti, S., and Pirinen, M. (2016). FINEMAP: efficient variable selection using summary data from genome-wide association studies. Bioinformatics *32*, 1493–1501.

22. Wang, G., Sarkar, A., Carbonetto, P., and Stephens, M. (2020). A simple new approach to variable selection in regression, with application to genetic fine mapping. J. R. Stat. Soc. Series B Stat. Methodol. *82*, 1273–1300.
23. Benner, C., Havulinna, A.S., Järvelin, M.R., Salomaa, V., Ripatti, S., and Pirinen, M. (2017). Prospects of Fine-Mapping Trait-Associated Genomic Regions by Using Summary Statistics from Genome-wide Association Studies. Am. J. Hum. Genet. *101*, 539–551.
24. Heyne, H.O., Karjalainen, J., Karczewski, K.J., Lemmelä, S.M., Zhou, W., FinnGen, Havulinna, A.S., Kurki, M., Rehm, H.L., Palotie, A., and Daly, M.J. (2023). Mono-and biallelic variant effects on disease at biobank scale. Nature *613*, 519–525.
25. Kanai, M., Ulirsch, J.C., Karjalainen, J., Kurki, M., Karczewski, K.J., Fauman, E., Wang, Q.S., Jacobs, H., Aguet, F., Ardlie, K.G., et al. (2021). Insights from complex trait fine-mapping across diverse populations. Preprint at medRxiv *1*. https://doi.org/10.1101/2021.09.03.21262975.
26. Kanai, M., Elzur, R., Zhou, W., Global Biobank Meta-analysis Initiative, Daly, M.J., Finucane, H.K., Hirbo, J.B., Wang, Y., Bhattacharya, A., Zhao, H., et al. (2022). Meta-analysis fine-mapping is often miscalibrated at single-variant resolution. Cell Genom. *2*, 100210.
27. Chen, W., Wu, Y., Zheng, Z., Qi, T., Visscher, P.M., Zhu, Z., and Yang, J. (2021). Improved analyses of gwas summary statistics by reducing data heterogeneity and errors. Nat. Commun. *12*, 7117.
28. Boyle, A.P., Hong, E.L., Hariharan, M., Cheng, Y., Schaub, M.A., Kasowski, M., Karczewski, K.J., Park, J., Hitz, B.C., Weng, S., et al. (2012). Annotation of functional variation in personal genomes using RegulomeDB. Genome Res. *22*, 1790–1797.
29. Wang, J., Huang, D., Zhou, Y., Yao, H., Liu, H., Zhai, S., Wu, C., Zheng, Z., Zhao, K., Wang, Z., et al. (2020). CAUSALdb: a database for disease/trait causal variants identified using summary statistics of genome-wide association studies. Nucleic Acids Res. *48*, D807–D816.
30. de Leeuw, C.A., Mooij, J.M., Heskes, T., and Posthuma, D. (2015). MAGMA: generalized gene-set analysis of GWAS data. PLoS Comput. Biol. *11*, e1004219.
31. Raulerson, C.K., Ko, A., Kidd, J.C., Currin, K.W., Brotman, S.M., Cannon, M.E., Wu, Y., Spracklen, C.N., Jackson, A.U., Stringham, H.M., et al. (2019). Adipose tissue gene expression associations reveal hundreds of candidate genes for cardiometabolic traits. Am. J. Hum. Genet. *105*, 773–787.
32. Giambartolomei, C., Vukcevic, D., Schadt, E.E., Franke, L., Hingorani, A.D., Wallace, C., and Plagnol, V. (2014). Bayesian test for colocalisation between pairs of genetic association studies using summary statistics. PLoS Genet. *10*, e1004383.
33. Zhu, Z., Zhang, F., Hu, H., Bakshi, A., Robinson, M.R., Powell, J.E., Montgomery, G.W., Goddard, M.E., Wray, N.R., Visscher, P.M., and Yang, J. (2016). Integration of summary data from GWAS and eQTL studies predicts complex trait gene targets. Nat. Genet. *48*, 481–487.
34. Finucane, H.K., Bulik-Sullivan, B., Gusev, A., Trynka, G., Reshef, Y., Loh, P.R., Anttila, V., Xu, H., Zang, C., Farh, K., et al. (2015). Partitioning heritability by functional annotation using genome-wide association summary statistics. Nat. Genet. *47*, 1228–1235.
35. Wang, Q.S., Kelley, D.R., Ulirsch, J., Kanai, M., Sadhuka, S., Cui, R., Albors, C., Cheng, N., Okada, Y., et al.; Biobank Japan Project (2021). Leveraging supervised learning for functionally informed fine-mapping of cis-eQTLs identifies an additional 20,913 putative causal eQTLs. Nat. Commun. *12*, 3394.
36. Weeks, E.M., Ulirsch, J.C., Cheng, N.Y., Trippe, B.L., Fine, R.S., Miao, J., Patwardhan, T.A., Kanai, M., Nasser, J., Fulco, C.P., et al. (2020). Leveraging polygenic enrichments of gene features to predict genes underlying complex traits and diseases. Preprint at medRxiv *1*. https://doi.org/10.1101/2020.09.08.20190561.
37. Bakker, O.B., Claringbould, A., Westra, H.-J., Wiersma, H., Boulogne, F., Võsa, U., Symmons, S.M., Jonkers, I.H., Franke, L., and Deelen, P. (2021). Linking common and rare disease genetics through gene regulatory networks. Preprint at medRxiv *1*. https://doi.org/10.1101/2021.10.21.21265342.
38. Gazal, S., Weissbrod, O., Hormozdiari, F., Dey, K.K., Nasser, J., Jagadeesh, K.A., Weiner, D.J., Shi, H., Fulco, C.P., O'Connor, L.J., et al. (2022). Combining SNP-to-gene linking strategies to identify disease genes and assess disease omnigenicity. Nat. Genet. *54*, 827–836.
39. Stouffer, S.A., Suchman, E.A., DeVinney, L.C., Shirley, A.S., and Williams, R.M. (1949). The american soldier: Adjustment during army life. Studies in Social Psychology in World War II 1.
40. Wallace, C. (2021). A more accurate method for colocalisation analysis allowing for multiple causal variants. PLoS Genet. *17*, e1009440.
41. Lehne, B., Lewis, C.M., and Schlitt, T. (2011). From SNPs to genes: disease association at the gene level. PLoS One *6*, e20133.
42. Aguet, F., Anand, S., Ardlie, K.G., Gabriel, S., Getz, G.A., Graubert, A., Hadley, K., Handsaker, R.E., Huang, K.H., Kashin, S., et al. (2020). The gtex consortium atlas of genetic regulatory effects across human tissues. Science *369*, 1318–1330.
43. Deelen, P., van Dam, S., Herkert, J.C., Karjalainen, J.M., Brugge, H., Abbott, K.M., van Diemen, C.C., van der Zwaag, P.A., Gerkes, E.H., Zonneveld-Huijssoon, E., et al. (2019). Improving the diagnostic yield of exome- sequencing by predicting gene-phenotype associations using large-scale gene expression analysis. Nat. Commun. *10*, 2837.
44. Piñero, J., Ramírez-Anguita, J.M., Saüch-Pitarch, J., Ronzano, F., Centeno, E., Sanz, F., and Furlong, L.I. (2020). The DisGeNET knowledge platform for disease genomics: 2019 update. Nucleic Acids Res. *48*, D845–D855.
45. Chen, E.Y., Tan, C.M., Kou, Y., Duan, Q., Wang, Z., Meirelles, G.V., Clark, N.R., and Ma'ayan, A. (2013). Enrichr: interactive and collaborative HTML5 gene list enrichment analysis tool. BMC Bioinf. *14*, 128.
46. Franz, M., Rodriguez, H., Lopes, C., Zuberi, K., Montojo, J., Bader, G.D., and Morris, Q. (2018). GeneMANIA update 2018. Nucleic Acids Res. *46*, W60–W64.
47. Mostafavi, S., and Morris, Q. (2010). Fast integration of heterogeneous data sources for predicting gene function with limited annotation. Bioinformatics *26*, 1759–1765.
48. Willems, E.L., Wan, J.Y., Norden-Krichmar, T.M., Edwards, K.L., and Santorico, S.A. (2020). Transethnic meta-analysis of metabolic syndrome in a multiethnic study. Genet. Epidemiol. *44*, 16–25.
49. Claussnitzer, M., Dankel, S.N., Kim, K.H., Quon, G., Meuleman, W., Haugen, C., Glunk, V., Sousa, I.S., Beaudry, J.L., Puviindran, V., et al. (2015). FTO Obesity Variant Circuitry and Adipocyte Browning in Humans. N. Engl. J. Med. *373*, 895–907.
50. Farh, K.K.H., Marson, A., Zhu, J., Kleinewietfeld, M., Housley, W.J., Beik, S., Shoresh, N., Whitton, H., Ryan, R.J.H., Shishkin, A.A., et al. (2015). Genetic and epigenetic fine mapping of causal autoimmune disease variants. Nature *518*, 337–343.

51. Gusev, A., Ko, A., Shi, H., Bhatia, G., Chung, W., Penninx, B.W.J.H., Jansen, R., de Geus, E.J.C., Boomsma, D.I., Wright, F.A., et al. (2016). Integrative approaches for large-scale transcriptome-wide association studies. Nat. Genet. *48*, 245–252.
52. Gamazon, E.R., Segrè, A.V., van de Bunt, M., Wen, X., Xi, H.S., Hormozdiari, F., Ongen, H., Konkashbaev, A., Derks, E.M., Aguet, F., et al. (2018). Using an atlas of gene regulation across 44 human tissues to inform complex disease- and trait-associated variation. Nat. Genet. *50*, 956–967.
53. Wainberg, M., Sinnott-Armstrong, N., Mancuso, N., Barbeira, A.N., Knowles, D.A., Golan, D., Ermel, R., Ruusalepp, A., Quertermous, T., Hao, K., et al. (2019). Opportunities and challenges for transcriptome-wide association studies. Nat. Genet. *51*, 592–599.
54. Sevillano, J., de Castro, J., Bocos, C., Herrera, E., and Ramos, M.P. (2007). Role of insulin receptor substrate-1 serine 307 phosphorylation and adiponectin in adipose tissue insulin resistance in late pregnancy. Endocrinology *148*, 5933–5942.
55. Wang, C., Mao, X., Wang, L., Liu, M., Wetzel, M.D., Guan, K.L., Dong, L.Q., and Liu, F. (2007). Adiponectin sensitizes insulin signaling by reducing p70 S6 kinase-mediated serine phosphorylation of IRS-1. J. Biol. Chem. *282*, 7991–7996.
56. Gao, H., Kim, Y.M., Chen, P., Igase, M., Kawamoto, R., Kim, M.K., Kohara, K., Lee, J., Miki, T., Ong, R.T.H., et al. (2013). Genetic variation in CDH13 is associated with lower plasma adiponectin levels but greater adiponectin sensitivity in East Asian populations. Diabetes *62*, 4277–4283.
57. Ding, B., Abe, J.I., Wei, H., Huang, Q., Walsh, R.A., Molina, C.A., Zhao, A., Sadoshima, J., Blaxall, B.C., Berk, B.C., and Yan, C. (2005). Functional role of phosphodiesterase 3 in cardiomyocyte apoptosis: implication in heart failure. Circulation *111*, 2469–2476.
58. Neville, M.J., Wittemans, L.B.L., Pinnick, K.E., Todorčević, M., Kaksonen, R., Pietiläinen, K.H., Luan, J., Scott, R.A., Wareham, N.J., Langenberg, C., and Karpe, F. (2019). Regional fat depot masses are influenced by protein-coding gene variants. PLoS One *14*, e0217644.
59. Levine, J.A., Jensen, M.D., Eberhardt, N.L., and O'Brien, T. (1998). Adipocyte macrophage colony-stimulating factor is a mediator of adipose tissue growth. J. Clin. Invest. *101*, 1557–1564.
60. Huang, X., Charbeneau, R.A., Fu, Y., Kaur, K., Gerin, I., MacDougald, O.A., and Neubig, R.R. (2008). Resistance to diet-induced obesity and improved insulin sensitivity in mice with a regulator of G protein signaling-insensitive G184S Gnai2 allele. Diabetes *57*, 77–85.
61. Riis-Vestergaard, M.J., Richelsen, B., Bruun, J.M., Li, W., Hansen, J.B., and Pedersen, S.B. (2020). Beta-1 and Not Beta-3 Adrenergic Receptors May Be the Primary Regulator of Human Brown Adipocyte Metabolism. J. Clin. Endocrinol. Metab. *105*, dgz298.
62. Finelli, C., and Tarantino, G. (2013). What is the role of adiponectin in obesity related non-alcoholic fatty liver disease? World J. Gastroenterol. *19*, 802–812.
63. Grömping, U. (2006). Relative importance for linear regression in r: The package relaimpo. J. Stat. Software *17*, 1–27.
64. Kurki, M.I., Karjalainen, J., Palta, P., Sipilä, T.P., Kristiansson, K., Donner, K.M., Reeve, M.P., Laivuori, H., Aavikko, M., Kaunisto, M.A., et al. (2023). Finngen provides genetic insights from a well-phenotyped isolated population. Nature *613*, 508–518.
65. Dalamaga, M., Diakopoulos, K.N., and Mantzoros, C.S. (2012). The role of adiponectin in cancer: a review of current evidence. Endocr. Rev. *33*, 547–594.
66. Pham, D.V., and Park, P.H. (2022). Adiponectin triggers breast cancer cell death via fatty acid metabolic reprogramming. J. Exp. Clin. Cancer Res. *41*, 9.
67. Pietzner, M., Wheeler, E., Carrasco-Zanini, J., Cortes, A., Koprulu, M., Wörheide, M.A., Oerton, E., Cook, J., Stewart, I.D., Kerrison, N.D., et al. (2021). Mapping the proteo-genomic convergence of human diseases. Science *374*, eabj1541.
68. Fauman, E.B., and Hyde, C. (2022). An optimal variant to gene distance window derived from an empirical definition of cis and trans protein QTLs. BMC Bioinf. *23*, 169.
69. Rondinone, C.M., Wang, L.M., Lonnroth, P., Wesslau, C., Pierce, J.H., and Smith, U. (1997). Insulin receptor substrate (IRS) 1 is reduced and IRS-2 is the main docking protein for phosphatidylinositol 3-kinase in adipocytes from subjects with non-insulin-dependent diabetes mellitus. Proc. Natl. Acad. Sci. USA *94*, 4171–4175.
70. Groeneveld, M.P., Brierley, G.V., Rocha, N.M., Siddle, K., and Semple, R.K. (2016). Acute knockdown of the insulin receptor or its substrates Irs1 and 2 in 3T3-L1 adipocytes suppresses adiponectin production. Sci. Rep. *6*, 21105.
71. Zhao, W., Rasheed, A., Tikkanen, E., Lee, J.-J., Butterworth, A.S., Howson, J.M.M., Assimes, T.L., Chowdhury, R., Orho-Melander, M., Damrauer, S., et al. (2017). Identification of new susceptibility loci for type 2 diabetes and shared etiological pathways with coronary heart disease. Nat. Genet. *49*, 1450–1457.
72. Yang, M., Qiu, S., He, Y., Li, L., Wu, T., Ding, N., Li, F., Zhao, A.Z., and Yang, G. (2021). Genetic ablation of C-reactive protein gene confers resistance to obesity and insulin resistance in rats. Diabetologia *64*, 1169–1183.
73. Hume, D.A., and MacDonald, K.P.A. (2012). Therapeutic applications of macrophage colony-stimulating factor-1 (CSF-1) and antagonists of CSF-1 receptor (CSF-1R) signaling. Blood *119*, 1810–1820.
74. Lin, W., Xu, D., Austin, C.D., Caplazi, P., Senger, K., Sun, Y., Jeet, S., Young, J., Delarosa, D., Suto, E., et al. (2019). Function of CSF1 and IL34 in Macrophage Homeostasis, Inflammation, and Cancer. Front. Immunol. *10*, 2019.
75. Carrero, J.A., McCarthy, D.P., Ferris, S.T., Wan, X., Hu, H., Zinselmeyer, B.H., Vomund, A.N., and Unanue, E.R. (2017). Resident macrophages of pancreatic islets have a seminal role in the initiation of autoimmune diabetes of NOD mice. Proc. Natl. Acad. Sci. USA *114*, E10418–E10427.
76. Bodle, C.R., Mackie, D.I., and Roman, D.L. (2013). RGS17: an emerging therapeutic target for lung and prostate cancers. Future Med. Chem. *5*, 995–1007.
77. Chang, D.C., Piaggi, P., Hanson, R.L., Knowler, W.C., Bucci, J., Thio, G., Hohenadel, M.G., Bogardus, C., and Krakoff, J. (2015). Use of a high-density protein microarray to identify autoantibodies in subjects with type 2 diabetes mellitus and an hla background associated with reduced insulin secretion. PLoS One *10*, e0143551.
78. Börjesson, M., Magnusson, Y., Hjalmarson, A., and Andersson, B. (2000). A novel polymorphism in the gene coding for the beta(1)-adrenergic receptor associated with survival in patients with heart failure. Eur. Heart J. *21*, 1853–1858.
79. Brodde, O.E. (2008). Beta-1 and beta-2 adrenoceptor polymorphisms: functional importance, impact on cardiovascular diseases and drug responses. Pharmacol. Ther. *117*, 1–29.
80. Cheng, J.B., Levine, M.A., Bell, N.H., Mangelsdorf, D.J., and Russell, D.W. (2004). Genetic evidence that the human

CYP2R1 enzyme is a key vitamin D 25-hydroxylase. Proc. Natl. Acad. Sci. USA *101*, 7711–7715.

81. Eliades, M., and Spyrou, E. (2015). Vitamin D: a new player in non-alcoholic fatty liver disease? World J. Gastroenterol. *21*, 1718–1727.
82. Huang, Y.-C., Chang, Y.-W., Cheng, C.-W., Wu, C.-M., Liao, W.-L., and Tsai, F.-J. (2020). Causal relationship between adiponectin and diabetic retinopathy: A mendelian randomization study in an asian population. Genes *12*, 17.
83. Ortega Moreno, L., Copetti, M., Fontana, A., De Bonis, C., Salvemini, L., Trischitta, V., and Menzaghi, C. (2016). Evidence of a causal relationship between high serum adiponectin levels and increased cardiovascular mortality rate in patients with type 2 diabetes. Cardiovasc. Diabetol. *15*, 17–26.
84. Uetani, E., Tabara, Y., Kawamoto, R., Onuma, H., Kohara, K., Osawa, H., and Miki, T. (2014). Cdh13 genotype–dependent association of high–molecular weight adiponectin with all-cause mortality: The j-shipp study. Diabetes Care *37*, 396–401.
85. Nielsen, M.B., Çolak, Y., Benn, M., and Nordestgaard, B.G. (2021). Low plasma adiponectin in risk of type 2 diabetes: observational analysis and one-and two-sample mendelian randomization analyses in 756,219 individuals. Diabetes *70*, 2694–2705.